Physical Properties of Cu Doped ZnO Nanocrystiline Thin Films

Nada K. Abbas [*]   *Zainab J. Shanan*   *Teeba H. Mohammed*

Department of Physics, College of science for Women, University of Baghdad , Baghdad, Iraq.
[*]Corresponding authors: nadabbs@yahoo.com[*], Zainabjassim73@yahoo.com , teeba.hussein912@yahoo.com
[*]ORCID ID: https://orcid.org/0000-0001-8573-4174 *, https://orcid.org/0000-0002-5166-5200

Abstract:

Thin films of ZnO nano crystalline doped with different concentrations (0, 6, 9, 12, and 18)wt. % of copper were deposited on a glass substrate via pulsed laser deposition method (PLD). The properties of ZnO: Cu thin-nanofilms have been studied by absorbing UV-VIS, X-ray diffraction (XRD) and atomic force microscopes (AFM). UV-VIS spectroscopy was used to determine the type and value of the optical energy gap, while X-ray diffraction was used to examine the structure and determine the size of the crystals. Atomic force microscopes were used to study the surface formation of precipitated materials. The UV-VIS spectroscopy was used to determine the type and value of the optical energy gap.

Keywords: Atomic force microscopy (AFM), Pulsed laser deposition (PLD), X-ray diffraction (XRD), ZnO:Cu nano crystalline.

Introduction:

Zinc oxide is an environmentally safe material, as it has a high binding energy at room temperature (60 meV) and also has a large direct energy gap (3.37 eV) [1-3] and thus can be used in various hardware applications , such as solar cells , smart windows, gas sensors, piezoelectric transducers, transparent high power electronics, varistors, and ultraviolet (UV) light-emitters[4–6]. Sub- Extra energy levels will be generated in the band gap of the semiconductors when it is doped with metal [7, 8]. Many minerals can assume valence depending on the surrounding chemicals, for example, any copper salt when doped in ZnO using an organic mineral solution can lead to various oxidation states Cu [9]. ZnO can be manufactured by several technologies such as chemical vapor deposition, thermal evaporation, magnetically splatter, pulse laser deposition (PLD), chemical vapor deposition, and non-vacuum methods can be used, i.e. absorption and interaction of the SILAR gel spin coating, Pyrolysis methods [1, 7, 10-17]. The PLD method is characterized by the other technologies, where in films were prepared by this method at low temperatures due to the increased energy of the lower particles in the laser column resulting from the relatively high deposition rates[16]. In this work, ZnO doped with copper films were prepared for this material of great importance in electro-optical applications [16]. PLD method has been used to prepare ZnO and ZnO:Cu films on glass substrates. Zinc oxide was doped with copper to reduce the band gap and to improve the properties of the solar cells.

Materials and Methods:

In the present study, thin films of ZnO: Cu were successfully deposited on glass substrates in the presence of oxygen gas, using pulsed laser deposition (PLD). The target of ZnO:Cu was prepared by mixing zinc acetate ($C_4H_6O_4Zn.2H_2O$), copper acetate $Cu(CH_3COO)_2$ and sodium hydroxide (NaOH) which were used without further purification. A solution of 0.3 M zinc acetate, 0.001 M copper acetate, and 1M sodium hydroxide were prepared in separated flasks. Cu doped ZnO with concentration 0, 6, 9, 12, and 18 wt. % nanoparticles were synthesized at room temperature in distilled water by the chemical precipitation method. The mixture is magnetically stirred for 30 min to get a homogeneous solution. Both the undoped and doped solutions are aged for one day for obtaining stability. The precipitation was washed with distilled water several times after separating it by filtration.Metallic ZnO-Cu target with different Cu concentrations (0, 6, 9, 12, and 18) wt. % was ablated by an Nd: YAG pulsed laser (Wavelength of laser: 1064/532 nm). The target with 500 no. of pulses, frequency 6 Hz, and energy

600 mJ were used for all samples. Films thickness was (166.25, 212.8, 160, 242, 170, and 177.3) nm for different concentration ratios using Optical Interferometer Method. The ZnO: Cu films were grown on 2.5 cm × 7.5 cm glass substrates. The crystal phase and crystallinity of the samples were investigated using X-ray diffraction for 2θ values ranging from 20 to 60∘ using Cu-Kα radiation (λ = 0.154nm). Transmittance spectra were recorded using UV- VIS spectrophotometer, while surface morphology has been obtained using atomic force microscopy (AFM). Van der Pauw (Ecopia HMS-3000) was used to measure the Hall Effect

Results and Discussion:

XRD Studies

The crystalline structures of pure ZnO and ZnO:Cu nanofilms deposited on glass substrates have been investigated using XRD

Figur 1 shows the X- ray diffraction (XRD) patterns of pure ZnO doped with Cu at different concentration samples. The diffraction peaks are indexed by comparing the data with JCPDS card file no.36-1451. The pattern of diffraction indicates thin films with a high degree were directed along (100) with c - axial direction in contrast to the study of R.K.Shukla et. al. [9] whose found the plane of 002 high intensity and have hexagonal crystal structures with low-intensity peaks correspond to the planes (002), (102), (101) and (110). In b pattern, a trace of an additional Cu-metal peak at 2θ of 36.26∘ was observed. This means that Cu atoms in these films (b pattern) not only acted as dopants but also formed embedded Cu clusters, which agrees well with a previous work [18].
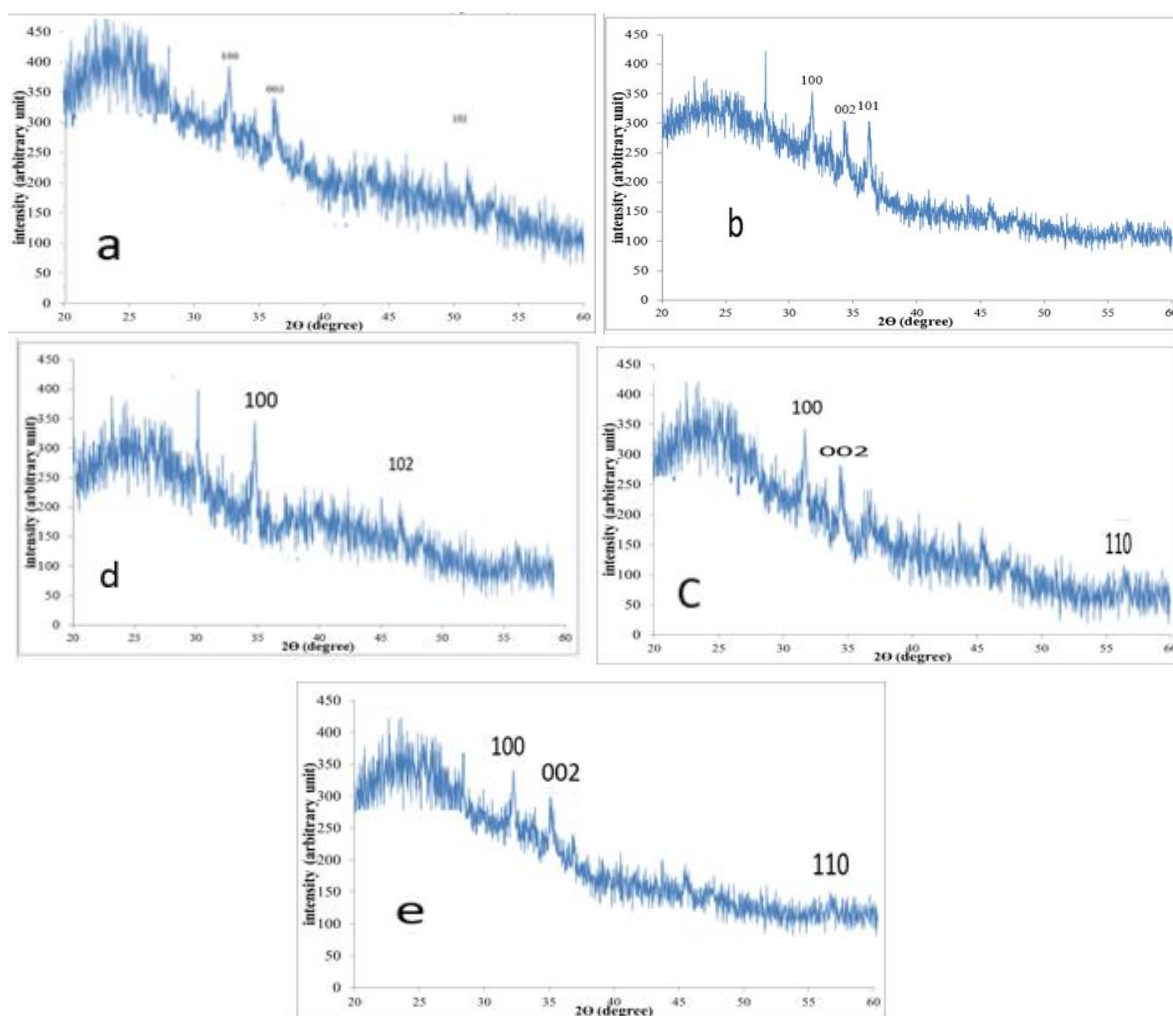

Figure 1. XRD spectrum of a: pure ZnO and doped ZnO with (b: 6, c: 9, d: 12, and e: 18) wt. % Cu thin films Deposited on glass substrate

The XRD patterns show a difference between the angular positions of Cu- doped ZnO thin films and those of undoped ZnO thin films. This can be attributed to the lattice mismatch induced by the difference between the lattice parameters of dopant atoms and that of the ZnO host.In addition we can see from Table 1 a slight shift in 2θ to higher value with increasing Cu content i.e., because the size of Cu ion (which have been inserted into lattice) is lesser than Zn ion (covalent radii for for Cu= 1.38Å) The XRD patterns described in this work correspond to those described in [19].

The full width at half maximum (FWHM) (The (FWHM) is calculated by calculating half of the wave height, then projecting two verticals lines on the x-axis (2θ) from the beginning and the end of the mid-width of the wave, then calculating ($\theta_2-\theta_1$), crystallites size (Cryst.S), and 2Θ of pure ZnO and ZnO doped with Cu thin films are listed in Table 1.

Table 1. XRD data of pure ZnO and ZnO doped with Cu.

Samples	2θ (Deg.)	FWHM (Deg.)	Cryst..S(nm)
Pure ZnO	31.4	0.002	72
	34.3	0.003	48.63
	47.4	0.002	76
6% Cu	31.77	0.005	28.87
	34.3	0.003	48.3
	36.26	0.004	36.47
9% Cu	31.2	0.003	48.13
	34.2	0.003	48.3
	57.3	0.002	79.6
12% Cu	31.5	0.003	47.8
	47.3	0.002	76.1
18% Cu	31.4	0.003	48.13
	34.5	0.002	72.6
	56.4	0.003	53.3

The crystallite size is calculated from XRD data by using Scherer formula eq.1. [20, 21]:

$$D= 0.9\lambda /\beta \cos\Theta \qquad 1$$

Where β is the full width at half maximum of the peaks, λ is the wavelength of incident X-ray (1.54 Å), D is the crystallite size, and Θ is the degree of the diffraction peak.

Surface Morphology

The AFM images of the surface morphologies of ZnO: Cu are shown in Fig. 2 (a, b, c, d, e, and f). The surface morphology of the ZnO:Cu thin films as observed from the AFM micrographs proves that the grains are uniformly distributed within the scanning area, with individual columnar grains extending upwards.

Open Access
Published Online First: July 2021

Baghdad Science Journal
2022, 19(1): 217-224

P-ISSN: 2078-8665
E-ISSN: 2411-7986
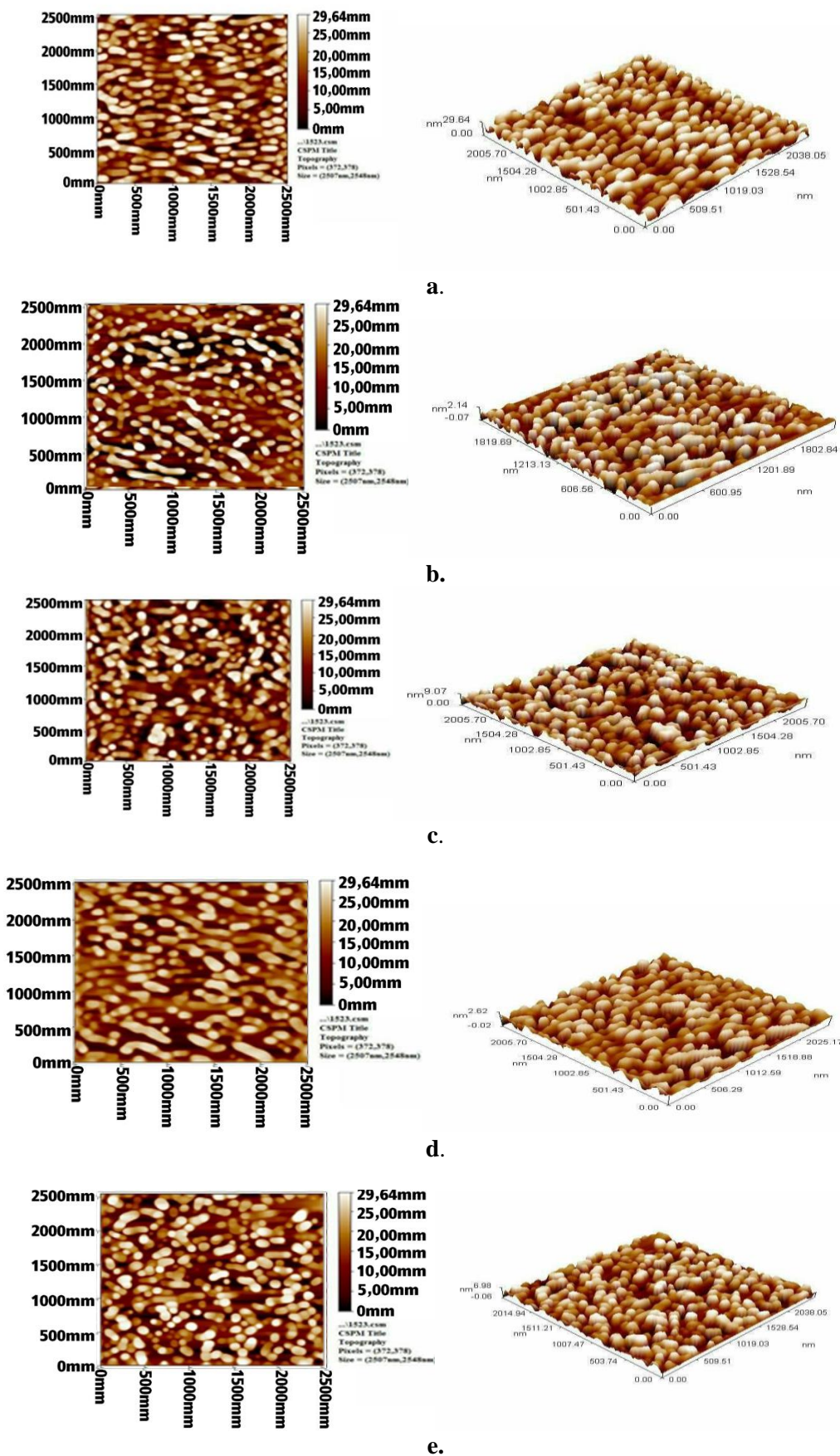
a.

b.

c.

d.

e.

Figure 2. AFM images describing the surface morphology for a: pure ZnO thin films and ZnO thin films doped with (b: 6, c: 9, d: 12, and e: 18) wt. % Cu.

Average grain size in diameter, Roughness Average, and Peak to peak of ZnO: Cu with concentration of Cu (0, 6, 9, 12, and 18) wt. % are displayed in Table 2.

Table 2. Grain size, average roughness, and Peak to peak of ZnO:Cu thin films.

Samples	Grain size (nm)	Roughness (nm)	Peak to peak(nm)
Pure ZnO	83.25	6.55	29.3
ZnO:Cu (6 wt. %)	70.63	0.553	2.21
ZnO:Cu (9 wt. %)	112.8	2.27	9.07
ZnO:Cu (12 wt. %)	78.66	0.525	2.54
ZnO:Cu (18 wt. %)	98.87	1.59	7.04

Figure 2 shows the atomic force microscopy (AFM) images of the pure ZnO and ZnO: Cu films. No pinholes were observed in the micrographs, indicating the successful deposition of compact films. As noted in Table 2, the root means square roughness (RMS) of the as-pure ZnO films is about 6.55 nm, which is in good agreement with that reported by Raied K. Jamal et al [21]. The grain size of the ZnO:Cu films decreases, as expected, before significantly increasing again at x=9%wt of Cu. It can be observed in Fig.2 and Table 2 that the grain size parallel to the surface is getting smaller, while the grain size vertical with the substrate is larger. The former reflects the (100) crystalline orientation, and the latter corresponds to the (002) crystalline orientation. Hence, the shift of the prominent crystal direction from (100) to (002) corresponds to the results obtained from XRD patterns.

Optical Properties
Absorption

Figure 3 illustrates the absorption spectra of ZnO:Cu nano crystalline from (400 – 700) nm. Red shift was observed for the doped zinc oxide thin films. This shift could be result due to the following reasons. The energy sub-levels for of the dopants lies below the conduction band edge (CBE) and above valence band edge (VBE) of ZnO. The creation of energy levels into the energy gap leads to a shift in band gap transmission and absorption visible light [20]. In addition, as the Cu content increased, the background absorption across the entire region increased. This may arise from the metallic Cu, which blocked most visible light.

When ZnO has been doped, the electron capture cases (the aperture) are created between the valance band edge and conduction band edge of

Zinc Oxide. ZnO doped with Cu films have been improved a visible light absorption.

Increasing visible absorption can be attributed to the transmission of the charge, which can be described as an alternative to the excitation of an electron from orbit d of metal ions [20].
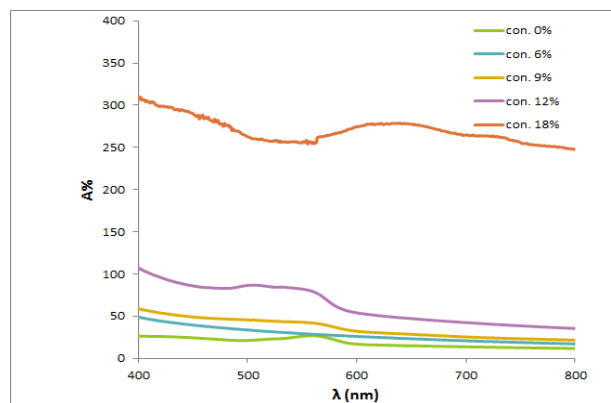Increased absorbance could be the result of increased levels of impurities within the energy gap [20].

Figure 3. Absorption spectra pure ZnO and ZnO Doped with (6, 9, 12,18) wt. %Cu thin films.

Transmission

The optical properties of the films deposited on glass substrates are determined from the absorbance (A), and transmittance (T) measurements in the range (300–1100) nm are shown in Fig. 4 , which illustrates the transmission spectra of ZnO and ZnO:Cu nanocrystalline with different concentrations in the range from 400 nm to 700 nm. It was found that the transmittance of ZnO:Cu films increased with the increase in the wavelength. It is clear from the same Figure that the transmittance decreases with increasing Cu concentration which can be also deduced from the changes in the films' colure. The transmission of doped ZnO was decreasing because the ionization energy of incident photons lies near the energy gap. This result is in agreement with the literature [20].
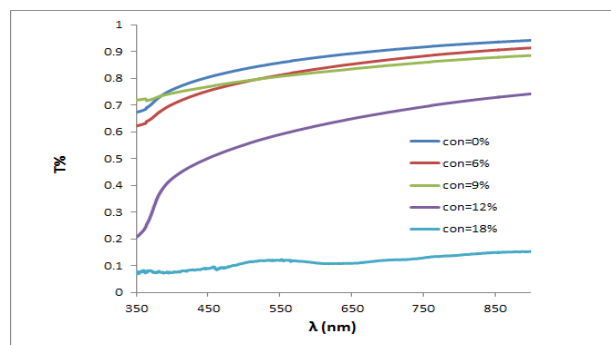

Figure 4. Optical transmission for the pure ZnO and ZnO: Cu thin films against wave length.

Energy Gap (Eg)

The type of transition was found to be direct (21). The optical energy gap values (Eg) for ZnO:Cu thin films prepared by PLD method have been determined from the region of the high absorption at the fundamental absorption edge of these films by using Tauc equation [21] eq.2

$$\alpha h\upsilon = A(h\upsilon - E_g)^r \quad \ldots\ldots\ldots\ldots \quad 2$$

where $h\upsilon$ is the photon energy, Eg is the optical energy gap, B is a constant depends on the nature of the material (properties of its valence and conduction band) and r ： is a constant that depends on the nature of the transition between the top of the valence band and bottom of the conduction band [22] . The bandgap values were determined from the intercept of the straight-line portion of the $(\alpha h\upsilon)^2$ against the hv which has been explained in Fig.5. When the concentration of doping increases the energy gap for thin films decreases due to the displacement of the absorption edge towards the higher wavelengths[23,24], which leads to a decrease in the energy gap of ZnO as shown in Table 3 These results are consistent with the results obtained by literature Ziad T. Al-Dahan [20]
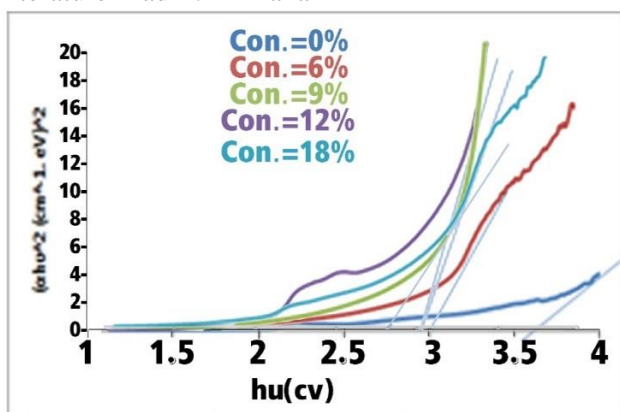

Figure 5. A plots of $(\alpha h\upsilon)^2$ verses photon energy (hv) of the pure ZnO and ZnO doped Cu thin films.

Table 3. List of the optical energy gaps of pure ZnO and ZnO: Cu films

Samples	E_g (eV)
Pure ZnO	3.6
ZnO:Cu (6 wt. %)	3.1
ZnO:Cu (9 wt. %)	3
ZnO:Cu (12 wt. %)	2.9
ZnO:Cu (18 wt. %)	2.8

Absorption Coefficient

The absorption coefficient α is determined from the high absorption area, i.e. at the fundamental absorption edge of the films using eq. 3 [25]. Absorption coefficient of the films was calculated from absorption (A) and the film thickness (t) using eq.3

$$\alpha = 2.303 \ A/ \ t \qquad\qquad 3$$

The absorption coefficient increases with increasing doping copper concentration as shown in Fig. 6. And these results agree with the result [26].
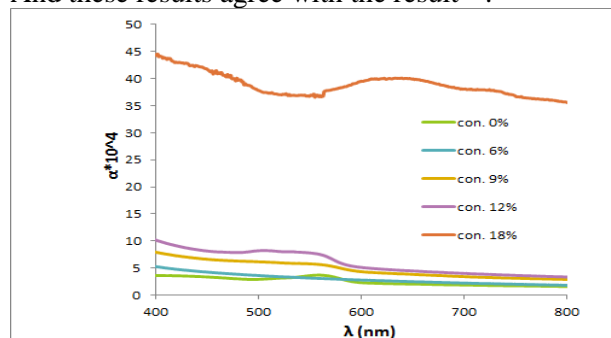

Figure 6. The Absorption coefficient spectra for the pure ZnO and ZnO Doped with (6, 9, 12, 18) wt. % Cu thin films against wavelength.

Electrical Properties:
Hall Effect Measurement

Hall effect calculations were performed at room temperature for pure zinc oxide films and doped with copper (6%, 9%, 12%, 18%) to determine the type and concentration of bulk carriers and their movement. The Hall coefficient (R_H) was a negative signal for pure and doped zinc oxide films suggesting that the films are n-type in conductivity. However, the impurity of the films sometimes affects the type of carriers at concentrations (12%, 18%) varying from (n-type to p-type). Carrier concentration N_H, mobility μ_H and type of charge carriers obtained from eqs. 3, 4, and 5 [26] are shown in Table 4 below respectively.

$$R_H = -1/n \ .q \ \text{for n-type} \qquad\qquad 4,$$
$$R_H = 1/p \ .q \ \text{for p-type} \qquad\qquad 5$$

From σ and R_H we may determine the hall mobility

$$\mu H = \sigma \ | \ R_H \ | \qquad\qquad 6$$

Table 4. Hall effect parameter of pure ZnO and ZnO: Cu films.

Content	R_H (cm³/C)	Σ (Ω.cm)$^{-1}$	μ_H (cm²/V.s)	N_H (cm^{-3})	tpye
Pure ZnO	-1.549E+6	2.115E-5	3.276E+1	-4.031E+12	N
ZnO:Cu (6 wt. %)	-1.071E+6	4.679E-5	5.009E+1	-5.831E+12	N
ZnO:Cu (9 wt. %)	-7.042E+5	2.075E-5	1.461E+1	-8.864E+12	N
ZnO:Cu (12 wt. %)	1.038E+6	2.138E-5	2.219E+1	6.012E+12	P
ZnO:Cu (18 wt. %)	4.421E+5	2.173E-5	9.608E+1	1.412E+12	P

From the Table we observe that the conductivity of pure ZnO and the ZnO doped with 6 and 9% Cu were the types of n while it became the type of p when doped with 12 and 18% of Cu. The Table shows that the values R_H, σ, and μ_H between the increase and decrease by increasing doped. And these results agree with the result [26]

Conclusion:

Nanocrystalline Cu doped ZnO films have been successfully deposited on glass substrates by pulsed laser deposition (PLD) and their structural and optical properties have been investigated. The XRD analysis demonstrates that the nanocrystals have a polycrystalline structure. The average size of the crystals is calculated and it is found that all samples have a nanoscale structure. The average thin film surface roughness has been increased and decreased with increasing Cu concentration. The values of the energy gap of prepared un-doped and ZnO doped with copper are found to be increasing with increasing Cu concentration. Hall measurements show that the conductivity type is transferred from type p to type n when the percentage of copper doping concentration is (12 and 18) %. From the results obtained, it is found that the prepared material can be used as a gas sensor and to improve the properties of solar cells in general and in the manufacture of photovoltaic cells in particular.

Authors' declaration:

- Conflicts of Interest: None.
- We hereby confirm that all the Figures and Tables in the manuscript are mine ours. Besides, the Figures and images, which are not mine ours, have been given the permission for re-publication attached with the manuscript.
- Ethical Clearance: The project was approved by the local ethical committee in University of Baghdad.

Authors' contributions statement:

Nada K. Abbas conceived of the presented idea. All authors contributed to the carried out the experiment to prepared the samples. Teeba H. Mohammed wrote the manuscript with support from Nada K. Abbas (Supervisor of the results of this work). All authors discussed the results and contributed to the final manuscript.

References

1. Abass N, Shanan Z, Mohammed T, Abbas L. Fabricated of Cu Doped ZnO Nanoparticles for Solar Cell Application. Baghdad Sic J 2018; 15: 2.
2. Pung S, Ong C, Mohd Isha K, Othman M.Synthesis and characterization of Cu-doped zno nanorods. Sains Malays. 2014; 43(2): 273–281.
3. Allabergenov B, Tursunkulov O, Abidov A, Choi A, Wook J, Kim S. Microstructural analysis and optical characteristics of Cu-doped ZnO thin films prepared by DC magnetron sputtering. J Cryst. Growth.2014; (2) 401: 573–576.
4. Nunes V, Souza A, Lima F, Oliveira G, FreireF, Almeida A. Effects of Potential Deposition on the Parameters of ZnO Dye-Sensitized Solar Cells. Mater Res. 2018; 2 (4):1- 8.
5. Shewale P, Patil V, Shin S, Kim J, Uplane M. H_2S gas sensing properties of nanocrystalline Cu-dopedZnO thin films prepared by advanced spray pyrolysis. Sensor Actuat B –Chem. 2013;186: 226–234.
6. Marin A, Mũnoz-Rojas D, Iza D, Gershon T, Musselman K, MacManus-Driscoll J. Novel atmospheric growth technique to improve both light absorption and charge collection in ZnO/Cu_2O thin film solar cells. Adv Funct Mater. 2013; 23(27): 3413–3419.
7. Musleh H, AlDahoudi N, Zayed H , Shaat S, Tamous H, Shurrab N, et al. Synthesis and Characterization of Zno Nanoparticles Using Hydrothermal and Sol-Gel Techniques for Dye-Sensitized Solar Cells. JUBES. 2018; 26: 9.
8. Acosta D, López-Suárez A, Magaña C, Hernández F. Structural, Electrical and Optical Properties of ZnO Thin Films Produced by Chemical Spray Using Ethanol in Different Amounts of the Sprayed Solution. Thin Solid Films.2018; 653 (1): 309-316.
9. Shukla R, Anchal S, Nishant K, Akhilesh P, Mamta P. Optical and Sensing Properties of Cu Doped ZnO Nanocrystalline thin Films. J Nanotechnol. 2015; 10.
10. Xu L, Xian F, Zheng G, Lai M. Realization of strong violet and blue emissions from ZnO thin flms by incorporation of Cu ions. Mater Res Bull. 2018; 99:144–151.
11. Kadam A, Kim T, Shin D, Garadkar K, Park J. Morphological evolution of Cu doped ZnO for enhancement of photocatalytic activity. J Alloy Compd. 2017;710: 102–113 .
12. Hsu L, Chen C,.Zhang X. Effect of the CU source on optical properties of CuZnO films deposited by ultrasonic spraying. Materials. 2014; 7(2):1261–1270.

13. Acosta D, López S, MagañaA, Hernández C. Structural, Electrical and Optical Properties of ZnO Thin Films Produced by Chemical Spray Using Ethanol in Different Amounts of The Sprayed Solution. Thin Solid Films. 2018;653(1): 309-316.

14. Pan F,Li J,Ma L. Electronic Structures and Ferromagnetism of Cu-Doped ZnO: the First-Principle Calculation Study. J. Super Cond. Novel Magnetism. 2018; 31: 2103–2110.

15. Younas M ,Shen J, He M,lortz R,Akhtar M,Ling F. Role of multivalent Cu, oxygen vacancies and CuO nanophase in the ferromagnetic properties of ZnO:Cu thin flms. Rsc Adv. 2015; 5: 55648–55657.

16. Niranjan K, Dutta S, Varghese S, Ray A, Barshilia H. Role of defects in one-step synthesis of Cu-doped ZnO nanocoatings by electrodeposition method with enhanced magnetic and electrical properties. Appl Phys A. 2017;123: 250.

17. Silambarasan M, Saravanan S, Soga T. Effect of Fe-Doping on The Structural, Morphological and Optical Properties of ZnO Nanoparticles Synthesized by Solution Combustion Process. Physica E: Low-dimensional Systems and Nanostructures. 2015; 71 (1): 109-116.

18. Jae-Ho Lee, Kwonwoo O, Kyungeun J, Wilson K, Man L. Tuning the Morphology and Properties of Nanostructured Cu-ZnO Thin Films Using a Two-Step Sputtering Technique. Met. 2020; 10: 437. doi:10.3390/met10040437

19. Krämer A, Engel S, Sangiorgi N, Sanson A, Bartolomé J, Gräf S, et al. ZnO Thin Films on Single Carbon Fibres Fabricated by Pulsed Laser Deposition (PLD). Appl Surf Sci.2017; 399 (1): 282-287.

20. Ziad T, Mohammed A. Growth and characterization of ZnO nanostructures using pulsed laser. J Opt.2013; 42:194–202

21. Shaveta T, Neha S, Anamika V, Jitender K. Structural and optical properties of copper doped ZnO nanoparticles and thin films. Adv Appl Sci Res. 2014; 5(4):18-24.

22. Abbas N, Ahlam M,Ruqayah A, Nagham Y. The effect of Copper Concentration on the Structural, Morphological and Optical Properties of CdS:Cu Nanocrystalline prepared by chemical bath deposition. Int J Eng Res. 2016; 7: 1.

23. Abbas N, Iqbal S, Alaa A. The effect of Selenium concentration on the structural , morphological and optical properties of CdSexS1-x thin films. IREPHY .2012; 6: 3.

24. Raied K., Iman N. Electrical properties of pure NiO and NiO:Au thin films prepared by ssdxusing pulsed laser deposition. I J P.2016; 14(29): 37-43.

25. Mott N, Davis E .Electronic Process in Non-Crystalline Materials"2nd ed. Oxford University Press,(1980).

26. Abbas N, Al-Rasoul T, Shanan Z. Structural and optical characterization of Cu and Ni doped ZnS nanoparticles. Int J Electrochem. Sci.2013; 8 (4): 5594-5604.

<div dir="rtl">

الخصائص الفيزيائية لا غشية اوكسيد الزنك النانوية المطعمة بالنحاس

طيبة حميد محمد   زينب جاسم شنان   ندى خضير عباس

قسم الفيزياء، كلية العلوم للبنات، جامعة بغداد، بغداد، العراق.

الخلاصة:

تم تصنيع اغشية أكسيد الزنك البلورية النانوية المطعمة بالنحاس (ZnO: Cu)بتراكيز مختلفة .. تم ترسيب (0 ، 6 ، 9 ، 12 ، 18) ٪ من النحاس على ركيزة زجاجية باستخدام تقنية ترسب الليزر النبضي (PLD) وبتراكيز مختلفة. وقد تم توصيف بلورات ZnO: Cu النانوية بواسطة أطياف UV-VIS ، حيود الأشعة السينية (XRD) ومجهر القوة الذرية (AFM). تم استخدام التحليل الطيفي للأشعة المرئية وفوق البنفسجية لتحديد نوع وقيمة فجوة الطاقة الضوئية ، بينما تم استخدام حيود الأشعة السينية لفحص الهيكل وتحديد حجم البلورات. تم استخدام مجاهر القوة الذرية لدراسة تكوين سطح المواد المترسبة. تم استخدام التحليل الطيفي للأشعة المرئية وفوق البنفسجية لتحديد نوع وقيمة فجوة الطاقة الضوئية .

الكلمات المفتاحية: مجهر القوة الذرية (AFM) ، ترسيب الليزر النبضي (PLD) ، حيود الأشعة السينية (XRD، ZnO: نانو بلوري.

</div>